

# Fabrication of a Continuous-Enfolded Grating by Ion-Beam–Sputter Deposition

## Introduction

The concept of depositing a corrugated multilayer dielectric reflector on a sinusoidal diffraction-grating surface as described by Li and Hirsh<sup>1</sup> is attractive for high-laser-damage applications since the diffraction grating does not contain contaminants from the grating patterning and etching processes, as is typical for multilayer dielectric diffraction gratings.<sup>1–4</sup> The concept behind such a grating is that each layer in the multilayer structure acts as a diffractive element, with the overall diffraction efficiency of the grating being the combined efficiency of all the layers. When such a device is fabricated, any patterning, etching, or replication to provide the surface relief is done on the substrate surface, with low-absorption materials then deposited to achieve high diffraction efficiency. In this manner, the incident laser light encounters only high-damage-threshold materials, having sufficiently reflected and/or diffracted before reaching any remaining organic materials at the substrate surface. The performance of such a structure can be calculated based on the electric-field contributions from each interface, taking into account the local curvature of the surface relief as demonstrated by Li.<sup>5</sup> The primary remaining challenge in such an approach is to improve the contour conformation of the coated dielectric layers, with traditional coating methods leading to a planarization of the surface relief, as illustrated in

Fig. 138.47(a) (Ref. 1). The goal in depositing such a coating is that each layer interface should have an identical surface relief, by depositing a consistent thickness over the surface structure regardless of the local orientation, as shown in Fig. 138.47(b).

Ion-beam sputtering (IBS) typically produces high-quality optical coatings, characterized by a dense film structure exhibiting low scatter and low absorption.<sup>6,7</sup> By using appropriate high-band-gap materials, IBS may produce high-quality films suitable for high-fluence laser applications.<sup>8</sup> In addition, IBS is based on the ablation of target material using a directional ion source, with film deposition resulting from well-characterized momentum transfer of the ions incident on the target surface. The resulting deposition source is of an extended-area, relative to evaporation sources that appear to be a point for sufficiently large deposition systems. In this manner, larger substrates may be coated with a directional deposition, rather than being limited by the extent of an evaporation source.

This effort describes a collimated IBS process and its application for depositing a conformal multilayer reflector over a sinusoidal diffraction grating. By conformally depositing alternating hafnia and silica dielectric layers to enhance a silver layer on a nominal 1740-lines/mm sinusoidal grating, a

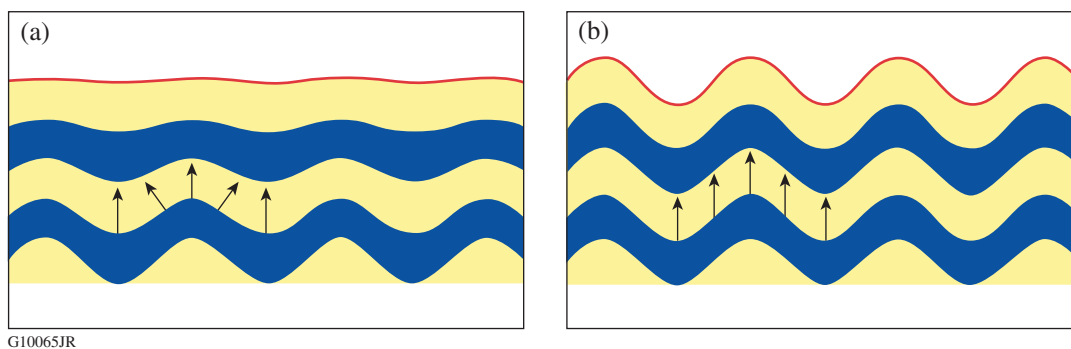


Figure 138.47

(a) Growth of the multilayer film over the grating normal to the *local* surface leads to rapid planarization of the grating structure. (b) Collimated deposition, with equal growth across the surface relief in the direction normal to the substrate plane, preserves the grating surface relief through the multilayer.

diffraction efficiency of 93% has been achieved for *p*-polarized light incident from the air surface. Laser-damage testing indicates that by using this type of structure, a 1-on-1 fluence of  $2.66 \pm 0.15 \text{ J/cm}^2$  can be achieved at 1053-nm,  $65^\circ$  incidence with a 10-ps pulse. Modifications will be necessary to deposit both the metal and dielectric layers in a single coating cycle, and further improvements calibrating the conformal structure will be pursued. The transfer function of the layered surface relief must be determined under different deposition conditions, but the demonstrated control suggests that continuous-enfolded gratings may be fabricated with high diffraction efficiency by using this method.

### Background

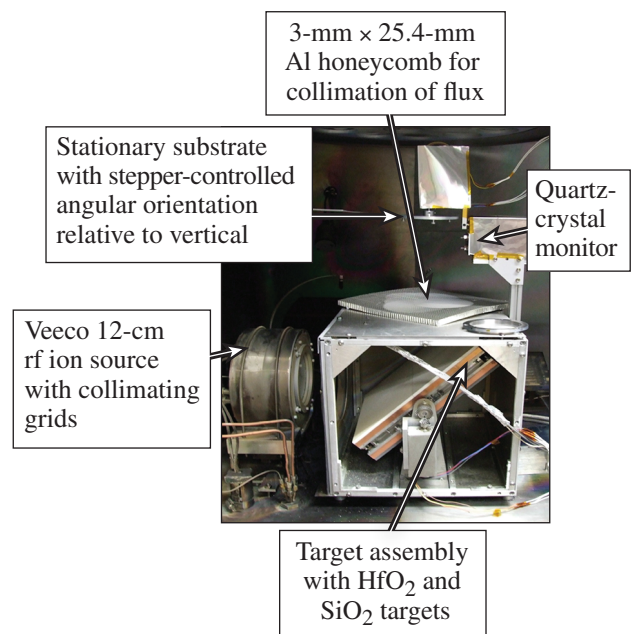
The basis of the continuous-enfolded grating structure is that the superposition of individual diffracted components from each layer in the multilayer coating results in overall high diffraction efficiency. The absorption present in a metallic coating limits the possible laser-damage threshold, so it is necessary to use a high-damage-threshold dielectric interference coating to limit the electric-field intensity striking the metal surface, increasing the overall laser-damage resistance of the diffraction grating. Each layer, however, must be conformally mapped to the surface beneath. Growth of a layer perpendicular to the local grating surface would rapidly planarize the grating structure; instead, the surface relief must be maintained in each layer, which is equivalent to uniform film growth perpendicular to the substrate surface without regard to the location or surface profile.

While evaporated coating processes can be designed to provide a uniform film thickness over a substrate surface, the angles of incidence on the substrate surface influence the relative thickness with a cosine dependence.<sup>9</sup> Furthermore, the source extent is generally quite small, limiting the region that may be coated with a collimated evaporant vapor flux. Sputtering processes make use of extended target sources that might be configured to provide an incident vapor flux of small angular extent, even over an extended substrate aperture. Control of the source distribution and/or the orientation of the substrate surface was considered to yield the desired deposition profile over a sinusoidal grating structure.

### Experimental Procedure

A single deposition system was not available to meet all needs in investigating this coating, so it was necessary to use three different coating chambers throughout this process: First, an MRC 902M magnetron sputtering system was used to deposit a layer of aluminum over a photoresist-patterned

grating to preserve the grating structure during epoxy replication. The aluminum film remained on the replicated grating, but the evaporation of an 80- to 100-nm-thick silver layer over the aluminum in a 54-in. coating chamber configured with a traditional planetary rotation was required to increase diffraction efficiency. This may also have the added benefit of preventing any remaining organic contaminants from the photoresist from being exposed to the incident laser intensity. The silver-coated replicated grating was then mounted in a custom 46-in. ion-beam-sputtering system equipped with a 12-cm Veeco radio-frequency (rf) ion source with converging grids, a rotatable target mount with hafnia and silica targets, a 25.4-mm-thick aluminum honeycomb filter with 3-mm hexagonal cells to collimate the vapor, and a stepper-motor-driven oscillating substrate mount as shown in Fig. 138.48. Coating thickness was controlled with a single quartz-crystal monitor.



G10067JR

Figure 138.48

Experimental ion-beam-sputtering system for depositing hafnia/silica multilayer coatings over a sinusoidal grating structure. The target assembly was rotated to select a hafnium-dioxide or silicon-dioxide target, while the grating substrate remained directly above the target, oscillating in a controlled manner to provide uniform coating distribution over the surface relief of the grating. rf: radio frequency.

The deposited-coating design is an enhanced silver reflector with seven dielectric layers deposited over the metal coating:

Al-coated grating / Ag / 0.9L HHLHL / air,

where  $L$  and  $H$  represent quarter-wave optical thicknesses at 1053 nm of silica and hafnia, respectively. This design provides a reflectance of greater than 99% at 1053 nm in  $p$  polarization over an angle range of  $62^\circ$  to  $72^\circ$ . The substrate is an epoxy-replicated sinusoidal grating with 1740 lines/mm and a depth of  $\sim 150$  nm, coated with an aluminum release layer (transferred from the original photoresist master grating). At this time we have not identified a method for cleaning the replicated grating, so deposition is performed on the aluminum, with potential contaminants remaining from the photoresist master grating. The opaque silver layer is evaporated while the substrate is rotated in a planetary rotation system. The IBS process is carried out with the substrate positioned directly above the source and oscillating to  $\pm 26^\circ$  from the incident vapor flux, with a 5-min dwell time at each end of the oscillation as shown in Fig. 138.49. The substrate continues to oscillate in this manner throughout the deposition of each layer, with average deposition times for individual layers being greater than 3 h.

Diffraction efficiency was measured with a 1053-nm laser source. Laser-damage testing was performed at 1053 nm with 10-ps pulses at  $66^\circ$  incidence in air with standard damage-test protocols.<sup>4</sup> Finally, the samples were cleaved and cross-section scanning electron microscopy was performed to characterize the conformal mapping of the coating to the underlying grating structure. Grating samples were mounted, coated with a thin layer of platinum, and imaged in a Zeiss 1530 scanning electron microscope (SEM), using in-lens secondary electron imaging as well as backscatter detection to enhance the contrast of the individual layers.

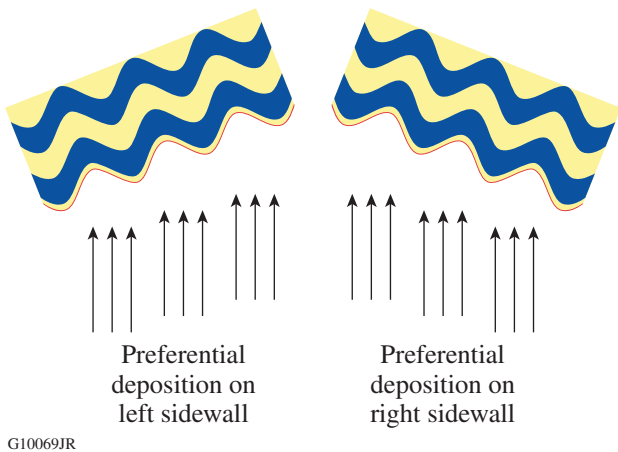


Figure 138.49 Oscillation of the grating surface relief to  $\pm\theta$  provides improved deposition on the grating sidewalls and reduced planarization.

## Results and Discussion

An evaporated coating deposition over a surface-relief grating was performed previously, confirming the challenges associated with coating over a grating structure as identified by Li and Hirsh.<sup>1,10</sup> A cross-sectional image is shown in Fig. 138.50(a), with a clear planarization within approximately eight layers.<sup>10</sup> The use of a collimated IBS process makes it possible to deposit a similar number of layers over a grating surface, but with a much higher degree of conformal mapping, as shown in Figs. 138.50(b)–138.50(e). The grating image in Fig. 138.50(b) results from a deposition without oscillation of the substrate above the source, showing greater deposited thickness in the minima of the grating profile and leading to sharper peaks in the maxima. The grating images in Figs. 138.50(c) and 138.50(d) also appear to have relatively sharp peaks, incorporating oscillation and honeycomb filtration, respectively, leading to a somewhat triangular shape in the grating profile. As seen in Fig. 138.50(e), this may be rounded somewhat by

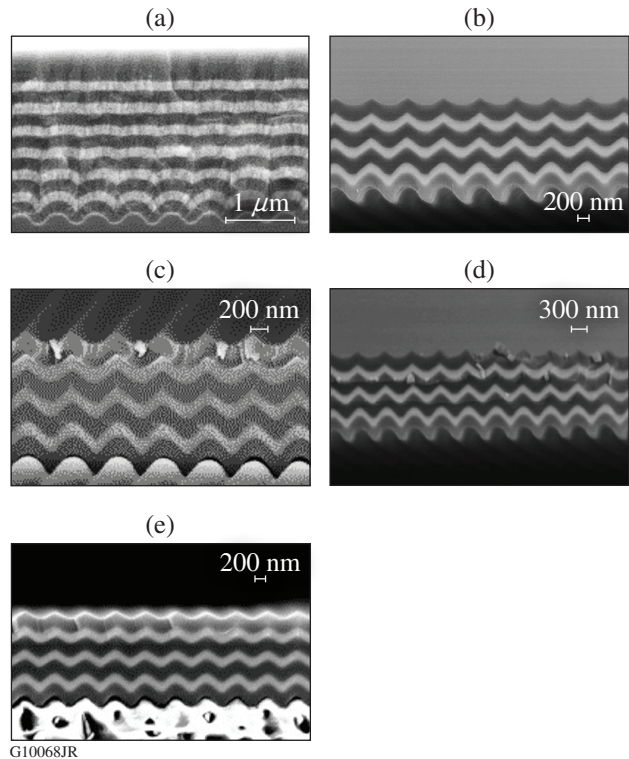


Figure 138.50 Scanning electron micrographs of multilayer interference coatings deposited over nominally sinusoidal diffraction-grating surfaces. The coating deposited by (a) electron-beam deposition quickly planarized, while (b) the IBS coating showed significant promise. The addition of (c) an aluminum honeycomb to improve vapor flux collimation, (d)  $\pm 26^\circ$  substrate oscillation, and (e) a  $0^\circ$  dwell in the tip-tilt substrate oscillations significantly improved the conformal properties of the coating deposition.

dwelling at a normal-incidence deposition position for 1 min between the 5-min depositions at  $\pm 26^\circ$  substrate orientation (as measured from normal-incidence vapor flux). Deposition with the relatively collimated IBS source on the stationary grating structure provides improved control of the film-growth direction, enabling one to fabricate a conformal multilayer structure.

The performance of the grating in Fig. 138.50(e) was evaluated for diffraction efficiency and laser-damage threshold. Given that the coating process was executed in three separate deposition systems and the epoxy replication process proved to be difficult, there were large regions of the 100-mm substrate where the coating delaminated from the epoxy surface. In the central region of the grating, however, there remained a test area with 93% diffraction efficiency and a 1-on-1 laser-damage threshold of  $2.66 \pm 0.15 \text{ J/cm}^2$  for 1053-nm,  $65^\circ$  incidence with a 10-ps pulse. For our initial effort, this result is quite encouraging since significant degradation of the laser-damage resistance is expected as the diffraction efficiency is decreased from the theoretical maximum of 98% for a sinusoidal continuous-enfolded grating at 1740 lines/mm. Such a degradation in efficiency leads to significant electric-field enhancement from multibeam interference of the incident, reflected, and diffracted components. Furthermore, this represents a significant improvement relative to the 84% diffraction efficiency reported by Li and Hirsh,<sup>1</sup> which required illumination from the substrate side of the grating, a configuration with negligible functionality for a high-fluence laser application.

To increase the utility of this grating fabrication technique, improved grating-performance modeling as a function of the profile of each layer is being pursued to determine the impact of deviations from a perfect sinusoidal shape. Control of variations in the conformal structure can be realized depending on the oscillation profile, particularly between the images in Figs. 138.50(c) and 138.50(e), where a normal-incidence deposition was added between each  $\pm 26^\circ$  deposition. Deposition perpendicular to the substrate surface can lead to planarization, given the high arrival energies of the ion-beam-sputtered flux, while deposition at high angles appears to lead to an alteration of the grating profile to more of a triangular or saw-toothed shape. The surface mobility of sputtered material can be significant for high arrival energies and impact at a glancing angle relative to the local substrate surface relief. By orienting the local surface relief normal to the incident flux, the mobility of arriving material can be limited.

The ideal grating shape must be determined for fabrication prior to the coating deposition, which, in conjunction with the transfer function of the coating process, determines the overall grating performance. Reactive ion etching, epoxy replication, and even direct coating of the developed photoresist grating are all possible means of fabricating a substrate with the appropriate surface-relief profile prior to deposition of the multilayer coating, but maintaining such a profile over large apertures is essential for developing a suitable production process. As larger substrates with high-quality surface relief become available, it is expected that a linear translation system will be incorporated to uniformly deposit over large apertures.

## Conclusions

A continuous-enfolded grating has been demonstrated with 93% diffraction efficiency and a laser-damage threshold of  $2.66 \pm 0.15 \text{ J/cm}^2$  at 1053-nm,  $65^\circ$  incidence in *p* polarization when tested in an *N*-on-1 configuration with a 10-ps pulse. The coating consists of a silver layer overcoated with ion-beam-sputtered hafnia and silica layers to provide greater than 99% reflectivity. SEM imaging shows good conformal mapping of the coating to the underlying grating structure, with available controls within the process to adjust the evolution of the grating profile throughout the layers. Efforts will continue to integrate the coating process in a single deposition system, better characterize the deposited film, develop a means to better clean the replicated grating prior to deposition, and expand the usable area of the coated grating. Improved modeling of the variations in the grating profile should lead to greater diffraction efficiency and laser-damage resistance.

## ACKNOWLEDGMENT

The authors express their appreciation to H. Huang for grating modeling and A. Kozlov for providing laser-damage-threshold measurements of the completed grating. This material is based upon work supported by the Department of Energy National Nuclear Security Administration under Award Number DE-NA0001944, the University of Rochester, and the New York State Energy Research and Development Authority. The support of DOE does not constitute an endorsement by DOE of the views expressed in this article.

## REFERENCES

1. L. Li and J. Hirsh, *Opt. Lett.* **20**, 1349 (1995).
2. J. A. Britten *et al.*, in *Laser-Induced Damage in Optical Materials: 1995*, edited by H. E. Bennett *et al.* (SPIE, Bellingham, WA, 1996), Vol. 2714, pp. 511–520.
3. M. D. Perry *et al.*, *Opt. Lett.* **20**, 940 (1995).

4. H. P. Howard, A. F. Aiello, J. G. Dressler, N. R. Edwards, T. J. Kessler, A. A. Kozlov, I. R. T. Manwaring, K. L. Marshall, J. B. Oliver, S. Papernov, A. L. Rigatti, A. N. Roux, A. W. Schmid, N. P. Slaney, C. C. Smith, B. N. Taylor, and S. D. Jacobs, *Appl. Opt.* **52**, 1682 (2013).
5. L. Li, *J. Opt. Soc. Am. A* **11**, 2816 (1994).
6. D. T. Wei and A. W. Louderback, U.S. Patent No. 4,142,958 (6 March 1979).
7. D. T. Wei, *Appl. Opt.* **28**, 2813 (1989).
8. X. Fu *et al.*, in *Laser-Induced Damage in Optical Materials: 2012*, edited by G. J. Exarhos *et al.* (SPIE, Bellingham, WA, 2012), Vol. 8530, Paper 85300X.
9. J. B. Oliver and D. Talbot, *Appl. Opt.* **45**, 3097 (2006).
10. J. B. Oliver, <http://www.optics.rochester.edu/workgroups/cml/opt307/spr04/jim/> (12 February 2014).